This full text paper was peer reviewed at the direction of IEEE Communications Society subject matter experts for publication in the IEEE ICC 2011 proceedings

On the Capacity of Quantized Gaussian MAC Channels with Finite Input Alphabet

Suresh Chandrasekaran, Saif K. Mohammed, and A. Chockalingam
Department of ECE, Indian Institute of Science, Bangalore 560012, INDIA

***Abstract*—In this paper, we investigate the achievable rate region of Gaussian multiple access channels (MAC) with finite input alphabet and *quantized output*. With finite input alphabet and an unquantized receiver, the two-user Gaussian MAC rate region was studied in [5]. In most high throughput communication systems based on digital signal processing, the analog received signal is quantized using a low precision quantizer. In this paper, we first derive the expressions for the achievable rate region of a two-user Gaussian MAC with finite input alphabet and *quantized output*. We show that, with finite input alphabet, the achievable rate region with the commonly used *uniform receiver quantizer* has a significant loss in the rate region compared to that in [5]. It is observed that this degradation is due to the fact that the received analog signal is densely distributed around the origin, and is therefore not efficiently quantized with a uniform quantizer which has equally spaced quantization intervals. It is also observed that the density of the received analog signal around the origin increases with increasing number of users. Hence, the loss in the achievable rate region due to uniform receiver quantization is expected to increase with increasing number of users. We, therefore, propose a novel *non-uniform quantizer* with finely spaced quantization intervals near the origin. For a two-user Gaussian MAC with a given finite input alphabet and low precision receiver quantization, we show that the proposed non-uniform quantizer has a significantly larger rate region compared to what is achieved with a uniform quantizer.**

Keywords *– Gaussian MAC, finite input alphabet, quantized receiver, discrete memoryless channel.*

I. Introduction

Most communication systems are based on digital signal processing, and rely on analog-to-digital converters (ADC) to digitize the analog received signal. With increasing throughput and bandwidth requirements, ADCs are expected to operate at high frequencies. However, at high operating frequencies, ADCs typically have low precision resulting in loss of system performance [1]. In [2], it has been shown that quantization causes floors in the bit error performance in single-input multiple-output (SIMO) fading channels. In [3], it is shown that for a single-input single-output (SISO) point-to-point single user system with additive white Gaussian noise (AWGN), receiver quantization with low precision ADC results in significant loss of capacity when compared to an unquantized receiver.

In this paper, we address the problem of degradation of the rate region of a two-user Gaussian multiple access channel (MAC) due to receiver quantization. In [3], the optimum input distribution for a point-to-point single-user SISO AWGN channel with quantized output was shown to be non-Gaussian with a finite support set. We, therefore, believe that even for a two-user Gaussian MAC with quantized output, the optimum input distribution for each user must have a finite support. In this paper, we do not derive the optimum input distribution for each user. Instead, we assume finite equi-probable input for each user, and derive expressions for the achievable rate region with a quantized receiver.

With finite input alphabets and an *unquantized* receiver, the two-user Gaussian MAC rate region has been studied in [5]. In [5], in terms of the achievable rate region, it was shown that, compared to having both the users transmit using the same finite signal set, it is better to have the second user transmit using a rotated version of the first user's signal set. We refer to the two-user Gaussian MAC system model in [5] (with finite input alphabet and no output quantization) as constellation constrained MAC (CCMAC).

In this paper, as in [5], we consider the rotation scheme, wherein one user transmits using a rotated version of the other user's signal set. However, instead of assuming an unquantized receiver as was done in [5], here we consider quantized receivers. Since *uniform* quantizers are commonly used in communication receivers, we first consider a uniformly quantized receiver, and show that with uniform quantization, there is a significant reduction in the two-user Gaussian MAC rate region compared to the CCMAC rate region. This is due to the fact that the received analog signal is densely distributed around the origin, and is therefore not efficiently quantized with a uniform quantizer.

This then motivates us to propose a novel *non-uniform* quantizer with finely spaced quantization intervals near the origin. We show that, with finite input alphabets and receiver quantization, the proposed non-uniform quantizer results in enlargement of the two-user Gaussian MAC rate region compared to that achieved with a uniform quantizer. It is further observed that, with increasing number of users, the probability distribution of the received analog signal is more and more dense around the origin. Hence, it is expected that with increasing number of users, larger enlargement in rate region can be achieved with non-uniform quantization compared to uniform quantization. The results and insights reported in this paper can be of relevance in the design of good low-precision quantizers at the receiver. We also believe that, to our knowledge, a study on the effect of output quantization in MAC channels with finite input alphabet have not been reported so far.

This work was supported in part by the DRDO-IISc Program on Advanced Research in Mathematical Engineering.

978-1-61284-231-8/11/$26.00 ©2011 IEEE

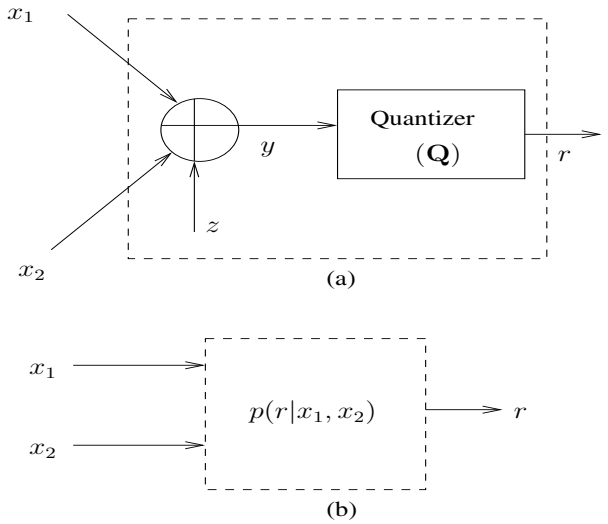

Fig. 1. (a) Two-user Gaussian MAC model with quantized output (b) Equivalent DMC.

II. System Model

Consider a two-user Gaussian MAC channel. Let x_1 and x_2 be the symbols transmitted by the first and second user, respectively. Let $x_1 \in \mathcal{X}_1$ and $x_2 \in \mathcal{X}_2$, where $\mathcal{X}_1$ and $\mathcal{X}_2$ are finite signal sets with N_1 and N_2 complex entries, respectively. Let $z \sim \mathcal{CN}(0, \sigma^2)$ be the additive white Gaussian noise at the receiver. The analog received signal is then given by

$$y = x_1 + x_2 + z. \tag{1}$$

The analog received signal, y, is quantized by a quantizer $\mathbf{Q}$, resulting in the output r, as shown in Fig. 1. The quantizer $\mathbf{Q}$ is actually composed of two similar quantizers acting independently on the real and imaginary components of the received analog signal, y. The real and imaginary components of the quantized output r are then given by

$$r^I = \mathbf{Q}_b(y^I), \quad r^Q = \mathbf{Q}_b(y^Q), \tag{2}$$

where the function $\mathbf{Q}_b(.)$ models a receiver quantizer having a resolution of b bits. $\mathbf{Q}_b(.)$ is a mapping from the set of real numbers $\mathbb{R}$ to a finite alphabet set $\mathcal{S}_b$ of cardinality 2^b, i.e.,

$$\mathbf{Q}_b : \mathbb{R} \mapsto \mathcal{S}_b, \quad \mathcal{S}_b \subset \mathbb{R}, \quad |\mathcal{S}_b| = 2^b. \tag{3}$$

Let $\mathcal{R}$ be defined as

$$\mathcal{R} = \{c + jd \mid c, d \in \mathcal{S}_b\}, \quad j = \sqrt{-1}. \tag{4}$$

Thus the quantized output, r, takes values from the set $\mathcal{R}$. Henceforth, we refer to the above system model of Gaussian MAC with finite input alphabet and receiver quantization as *quantized MAC (QMAC)*.

III. Rate Region of Two-User QMAC

In this section, we derive analytical expressions for the rate region of a two-user QMAC. From the Fig. 1, we observe that the effective multiple-access channel after receiver quantization, $(\mathcal{X}_1 \times \mathcal{X}_2,\, p(r|x_1, x_2),\, \mathcal{R})$, is a discrete memoryless channel (DMC) with the transition probabilities derived and given in (10). Let R_1 and R_2 represent the rates achieved by user 1 and user 2, respectively. Since QMAC is a discrete memoryless multiple-access channel, the achievable rate region [4] is the set of all rate pairs (R_1, R_2) satisfying

$$\begin{aligned} R_1 &\leq I(x_1 : r \,|\, x_2) && (5)\\ R_2 &\leq I(x_2 : r \,|\, x_1) && (6)\\ R_1 + R_2 &\leq I(x_1, x_2 : r) \\ &= I(x_2 : r) + I(x_1 : r \,|\, x_2). && (7) \end{aligned}$$

The mutual information $I(x_2 : r)$, $I(x_1 : r|x_2)$ are given by

$$\begin{aligned} I(x_2 : r) &= H(r) - H(r|x_2) && (8)\\ I(x_1 : r|x_2) &= H(r|x_2) - H(r|x_1, x_2), && (9) \end{aligned}$$

where the entropies in (8) and (9) are calculated using the probability distribution function

$$\begin{aligned} &p\left(r = \mathcal{S}_b(i) + j\mathcal{S}_b(k) \,|\, x_1 = \mathcal{X}_1(l), x_2 = \mathcal{X}_2(m)\right) \\ &= p(r^I = \mathcal{S}_b(i),\, r^Q = \mathcal{S}_b(k) \,|\, x_1 = \mathcal{X}_1(l), x_2 = \mathcal{X}_2(m)) \\ &= p(z^I \in \mathcal{F}(\mathcal{X}_1^I(l), \mathcal{X}_2^I(m), \mathcal{S}_b(i))) \\ &\qquad \times p(z^Q \in \mathcal{F}(\mathcal{X}_1^Q(l), \mathcal{X}_2^Q(m), \mathcal{S}_b(k))), \quad (10) \end{aligned}$$

where $j = \sqrt{-1}$, and $\mathcal{S}_b(i)$, $\mathcal{X}_1(i)$ and $\mathcal{X}_2(i)$ refer to the ith element of sets $\mathcal{S}_b$, $\mathcal{X}_1$ and $\mathcal{X}_2$, respectively. $\mathcal{X}_1^I(l)$, $\mathcal{X}_1^Q(l)$ and $\mathcal{X}_2^I(m)$, $\mathcal{X}_2^Q(m)$ are the real and imaginary parts of $\mathcal{X}_1(l)$ and $\mathcal{X}_2(m)$, respectively.

The region $\mathcal{F}(.)$ is defined as

$$\mathcal{F}(p, q, t) = \{n \in \mathbb{R} \,|\, \mathbf{Q}_b(p + q + n) = t\}, \tag{11}$$

and $n \sim \mathcal{N}(0, \sigma^2/2)$. From (10), the probability distributions $p(r|x_2)$ and $p(r)$ are calculated as

$$\begin{aligned} &p(r = \mathcal{S}_b(i) + j\mathcal{S}_b(k) \,|x_2 = \mathcal{X}_2(m)) \\ &= \frac{1}{N_1} \sum_{l=1}^{N_1} p(r = \mathcal{S}_b(i) + j\mathcal{S}_b(k) | x_1 = \mathcal{X}_1(l), x_2 = \mathcal{X}_2(m)); \quad (12) \end{aligned}$$

$$\begin{aligned} &p(r = \mathcal{S}_b(i) + j\mathcal{S}_b(k)) \\ &= \frac{1}{N_2} \sum_{m=1}^{N_2} p(r = \mathcal{S}_b(i) + j\mathcal{S}_b(k) | x_2 = \mathcal{X}_2(m)). \quad (13) \end{aligned}$$

On substituting (10), (12), (13) into (8) and (9), $I(x_2 : r)$ and $I(x_1 : r|x_2)$ can be computed. By symmetry, $I(x_1 : r)$ and $I(x_2 : r|x_1)$ can be computed in a similar manner. The final expressions for the achievable rate pairs (R_1, R_2) are then given by (14), (15), and (16), presented on the top of the next page.

Now, let $\mathbb{A}_M \stackrel{\triangle}{=} \{-(M-1), \cdots, -1, 1, \cdots, (M-1)\}$ be the M-PAM signal set, and $\mathbb{A}_{M^2} \stackrel{\triangle}{=} \{u + jv \mid u, v \in \mathbb{A}_M\}$ denote the corresponding M^2-QAM signal set. We restrict the input of the first user to be from M^2-QAM alphabet, and the second user input to be from a rotated version of the first user's input alphabet, i.e., $\mathcal{X}_1 = \mathbb{A}_{M^2}$, and

$$\mathcal{X}_2 \stackrel{\triangle}{=} \{u\, e^{j\theta} \mid u \in \mathcal{X}_1\}, \tag{17}$$

where θ is the rotation angle. We are interested in maximizing the sum rate $(R_1 + R_2)$ achieved using the input alphabets

$$R_1 \leq \log_2(N_1) - \frac{1}{N_1 N_2} \sum_{i=1}^{2^b} \sum_{k=1}^{2^b} \sum_{l_1=1}^{N_1} \sum_{m_1=1}^{N_2} p_{r|x_1,x_2}(\mathcal{S}_b(i)+j\mathcal{S}_b(k) \mid \mathcal{X}_1(l_1), \mathcal{X}_2(m_1)) \times \log_2 \left\{ \frac{\sum_{l_2=1}^{N_1} p_{r|x_1,x_2}(\mathcal{S}_b(i)+j\mathcal{S}_b(k) \mid \mathcal{X}_1(l_2), \mathcal{X}_2(m_1))}{p_{r|x_1,x_2}(\mathcal{S}_b(i)+j\mathcal{S}_b(k) \mid \mathcal{X}_1(l_1), \mathcal{X}_2(m_1))} \right\} \quad (14)$$

$$R_2 \leq \log_2(N_2) - \frac{1}{N_1 N_2} \sum_{i=1}^{2^b} \sum_{k=1}^{2^b} \sum_{l_1=1}^{N_1} \sum_{m_1=1}^{N_2} p_{r|x_1,x_2}(\mathcal{S}_b(i)+j\mathcal{S}_b(k) \mid \mathcal{X}_1(l_1), \mathcal{X}_2(m_1)) \times \log_2 \left\{ \frac{\sum_{m_2=1}^{N_2} p_{r|x_1,x_2}(\mathcal{S}_b(i)+j\mathcal{S}_b(k) \mid \mathcal{X}_1(l_1), \mathcal{X}_2(m_2))}{p_{r|x_1,x_2}(\mathcal{S}_b(i)+j\mathcal{S}_b(k) \mid \mathcal{X}_1(l_1), \mathcal{X}_2(m_1))} \right\} \quad (15)$$

$$R_1 + R_2 \leq \log_2(N_1 N_2) - \frac{1}{N_1 N_2} \sum_{i=1}^{2^b} \sum_{k=1}^{2^b} \sum_{l_1=1}^{N_1} \sum_{m_1=1}^{N_2} p_{r|x_1,x_2}(\mathcal{S}_b(i)+j\mathcal{S}_b(k) \mid \mathcal{X}_1(l_1), \mathcal{X}_2(m_1)) \times \log_2 \left\{ \frac{\sum_{l_2=1}^{N_1} \sum_{m_2=1}^{N_2} p_{r|x_1,x_2}(\mathcal{S}_b(i)+j\mathcal{S}_b(k) \mid \mathcal{X}_1(l_2), \mathcal{X}_2(m_2))}{p_{r|x_1,x_2}(\mathcal{S}_b(i)+j\mathcal{S}_b(k) \mid \mathcal{X}_1(l_1), \mathcal{X}_2(m_1))} \right\} \quad (16)$$

$\mathcal{X}_1$ and $\mathcal{X}_2$ defined above. Since R_1 and R_2 are functions of θ, we denote them by $R_1(\theta)$ and $R_2(\theta)$, respectively. For a given b-bit quantizer, the optimal rotation angle, θ^{opt}, which maximizes the sum rate is given by

$$\theta^{opt} = \arg \max_{\{\theta | \mathcal{X}_1 \in \mathbb{A}_{M^2}, \mathcal{X}_2 \in \{ue^{j\theta} | u \in \mathcal{X}_1\}\}} R_1(\theta) + R_2(\theta). \quad (18)$$

In all the numerical results reported in sections IV and V, the resolution of θ in the above optimization is set to 1°.

IV. QMAC with Uniform Quantizer

In this section, we study the achievable two-user QMAC rate region with a uniform b-bit quantizer. First, define the sum signal set as

$$\mathcal{X}_{sum} = \{x_1 + x_2 \,|\, x_1 \in \mathcal{X}_1,\, x_2 \in \mathcal{X}_2\}. \quad (19)$$

Let X^I and X^Q be defined as

$$X^I \triangleq \max_{a \in \mathcal{X}_{sum}} |a^I|, \quad X^Q \triangleq \max_{a \in \mathcal{X}_{sum}} |a^Q|. \quad (20)$$

Now, the function $\mathbf{Q}_b(.)$ for the uniform b-bit quantizer on the real component of the received signal y is given by

$$r^I = \mathbf{Q}_b(y^I) \triangleq \begin{cases} +1, & \zeta(y^I) > (2^{b-1}-1) \\ -1, & \zeta(y^I) < -(2^{b-1}-1) \\ \dfrac{2\zeta(y^I)+1}{2^b-1}, & \text{otherwise,} \end{cases} \quad (21)$$

where $\zeta(y^I) \triangleq \left\lfloor \frac{y^I}{X^I} \frac{(2^b-1)}{2} \right\rfloor$. Similarly, for the imaginary component of y,

$$r^Q = \mathbf{Q}_b(y^Q) \triangleq \begin{cases} +1, & \zeta(y^Q) > (2^{b-1}-1) \\ -1, & \zeta(y^Q) < -(2^{b-1}-1) \\ \dfrac{2\zeta(y^Q)+1}{2^b-1}, & \text{otherwise,} \end{cases} \quad (22)$$

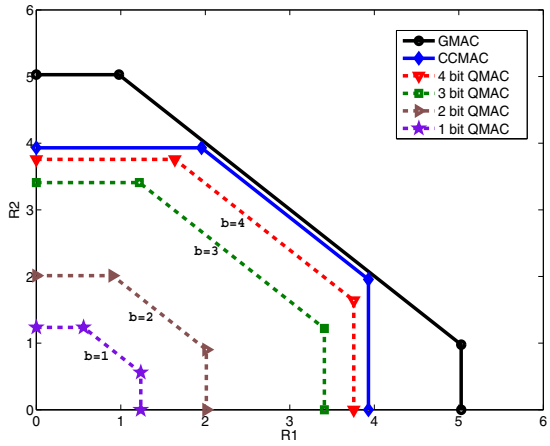

Fig. 2. Rate region of two-user QMAC with uniform quantizer. User 1 transmits from 16-QAM signal set, and User 2 transmits from an optimally rotated version of the first user's signal set. SNR per user = 15 dB.

where $\zeta(y^Q) \triangleq \left\lfloor \frac{y^Q}{X^Q} \frac{(2^b-1)}{2} \right\rfloor$.

With the uniform quantizer defined in (21) and (22), we have numerically evaluated the rate region using (14),(15) and (16), the results of which are discussed next.

A. Results and Discussion

In Fig. 2, we plot the rate region of a two-user QMAC as a function of the quantizer resolution, b, with User 1 using a 16-QAM input alphabet and User 2 using an optimally rotated version of the 16-QAM alphabet, as per (18), at SNR per user = 15 dB. The rate regions of GMAC (Gaussian MAC with Gaussian inputs and no output quantization) and CCMAC (Gaussian MAC with finite input and no output quantization [5]) are also plotted. From Fig. 2, we observe that with low precision ADCs ($b = 1$ or 2 bits), the sum rate achieved with uniform receiver quantization is very

poor compared to the sum rate of CCMAC. For instance, with a 2-bit uniform quantizer, the sum rate is 2.9144 bits which is just 49.5% of the sum rate of CCMAC (5.886 bits). To achieve a sum rate close to CCMAC, increased quantization resolution is required. For a fixed quantization resolution of b bits, the degradation in the rate region due to a uniform quantizer compared to CCMAC is expected to be more with increasing number of users. This is because the sum constellation becomes more and more dense around the origin, as illustrated in Fig. 3. Figure 3(a) shows the two-user sum signal set with User 1 using 16-QAM with no rotation and User 2 using 16-QAM with 45° rotation. Figure 3(b) shows the three-user sum signal set; User 1 using 16-QAM with no rotation and Users 2 and 3 using 16-QAM with 30° and 60° rotations, respectively. It can be seen that the scatter plot for the three-user sum signal set is clustered more around the origin than that for the two-user sum signal set.

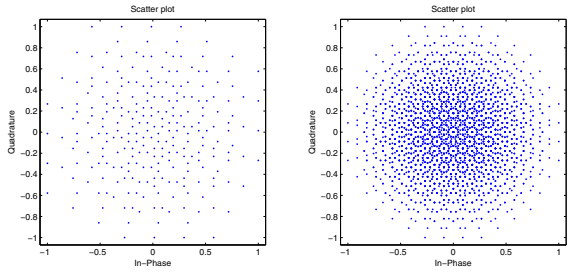

(a) 2-user sum signal set (b) 3-user sum signal set

Fig. 3. Scatter plots of two-user and three-user sum signal sets.

B. Motivation for a Non-uniform Quantizer

Since the symbols in the sum signal set are densely distributed around the origin, for a given quantization resolution of b bits, the uniform quantizer may not be the best quantizer in terms of the achievable rate region. We highlight this point through a simple example. Let

$$\left(\frac{x_1^I + x_2^I}{X^I}\right) \in \left\{-1, \frac{-7}{15}, \frac{-3}{15}, \frac{-1}{15}, \frac{1}{15}, \frac{3}{15}, \frac{7}{15}, 1\right\}. \quad (23)$$

As illustrated in Figure 4(a), with a $b = 3$-bit uniform quantizer, the receiver is unable to distinguish between the transmitted points t_1 and t_2, since they both fall in the same quantization interval. It is expected that a quantizer which can distinguish between all possible transmitted points would have a better rate region than a quantizer which fails to do so. Hence, as shown in Fig. 4(b), with $b = 3$ bits, a non-uniform quantizer, which distinguishes between all possible transmitted points, would have a better rate region than what is achieved by a $b = 3$ bit uniform quantizer. In the following section, we propose a non-uniform quantizer for QMAC. We will see that indeed the proposed non-uniform quantizer enlarges the rate region.

V. A Non-uniform Quantizer for QMAC

In this section, we propose a non-uniform quantizer for QMAC. The function $\mathbf{Q}_b(.)$ for the real component of the received signal in the proposed non-uniform quantizer is

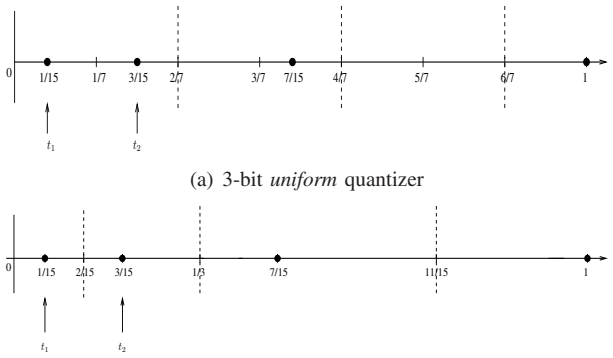

(a) 3-bit *uniform* quantizer

(b) 3-bit *non-uniform* quantizer

Fig. 4. Plot of the quantization intervals for 3-bit uniform and non-uniform quantizers. The boundaries between the quantization regions are demarcated by the dotted lines and the black dots show the points given in (23). Since the quantizer is symmetric about the origin, only the positive side is shown.

$$r^I = \mathbf{Q}_b(y^I) \triangleq \begin{cases} +1, & \zeta(y^I) > (2^{b-1}-1) \\ -1, & \zeta(y^I) < -(2^{b-1}-1) \\ \frac{1}{2}\left[\left(\frac{2\zeta(y^I)}{2^b-1}\right)^p + \left(\frac{2(\zeta(y^I)+1)}{2^b-1}\right)^p\right], & \text{o.w.,} \end{cases} \quad (24)$$

where $p \geq 1$, $\zeta(y^I) \triangleq \left\lfloor \left(\frac{2^b-1}{2}\right)\left(\frac{y^I}{X^I}\right)^{1/p} \right\rfloor$ and X^I defined in (20).

Likewise, for the imaginary component

$$r^Q = \mathbf{Q}_b(y^Q) \triangleq \begin{cases} +1, & \zeta(y^Q) > (2^{b-1}-1) \\ -1, & \zeta(y^Q) < -(2^{b-1}-1) \\ \frac{1}{2}\left[\left(\frac{2\zeta(y^Q)}{2^b-1}\right)^p + \left(\frac{2(\zeta(y^Q)+1)}{2^b-1}\right)^p\right], & \text{o.w.} \end{cases} \quad (25)$$

where $\zeta(y^Q) \triangleq \left\lfloor \left(\frac{2^b-1}{2}\right)\left(\frac{y^Q}{X^Q}\right)^{1/p} \right\rfloor$ and X^Q defined in (20).

Note that the parameter p in (24) and (25), is a quantizer design parameter, which is used to increase/decrease the quantization granularity around the origin. It can be seen that the uniform quantizer in (21), (22) is a special case of this non-uniform quantizer with $p = 1$.

For a *fixed* rotation angle θ and a quantizer resolution of b bits, the sum rate $R_1(\theta)+R_2(\theta)$ is a function of the parameter p. Since the sum rate is a function of both p and θ, we shall denote it by

$$R_{sum}(\theta, p) = R_1(\theta, p) + R_2(\theta, p). \quad (26)$$

For a fixed θ, the optimal quantizer parameter, $p^*(\theta)$, which maximizes the sum rate is given by

$$p^*(\theta) = \arg \max_{p:\, p \geq 1} R_{sum}(\theta, p). \quad (27)$$

In the following subsection, for a fixed θ, we present a low-complexity iterative algorithm to find a suboptimum solution to the maximization problem in (27).

A. An Iterative Algorithm to Solve (27)

Let $p^{(k)}$ and $R^{(k)} = R_{sum}(\theta, p^{(k)})$ denote the value of p and the sum rate in the kth iteration, respectively. The algorithm

starts with $p^{(0)} = 1$. In the $(k+1)$th iteration, evaluate $\tilde{R}^{(k+1)} = R_{sum}(\theta, p^{(k)}+1)$. If $\tilde{R}^{(k+1)} \geq R^{(k)}$, then go to the next iteration with $R^{(k+1)} = \tilde{R}^{(k+1)}$ and $p^{(k+1)} = p^{(k)} + 1$. If $\tilde{R}^{(k+1)} < R^{(k)}$, then evaluate (26) for all values of p in the set

$$P = \left\{ p^{(k)} + l\Delta,\ l \in \left\{ \left\lfloor \frac{-1}{\Delta} \right\rfloor, \cdots, -1, 0, 1, \cdots, \left\lfloor \frac{1}{\Delta} \right\rfloor \right\} \subset \mathbb{Z} \right\}, \tag{28}$$

where $\Delta < 1$ is the search granularity of the algorithm. Find

$$\tilde{l} = \arg \max_{l \in \left\{ \left\lfloor \frac{-1}{\Delta} \right\rfloor, \cdots, 0, \cdots, \left\lfloor \frac{1}{\Delta} \right\rfloor \right\}} R_{sum}(\theta, p^{(k)} + l\Delta). \tag{29}$$

Output $\tilde{p}(\theta) = p^{(k)} + \tilde{l}\Delta$ as the solution and stop.

In the above, the algorithm iteratively increments p in steps of one until the sum rate cannot be further increased after some iteration k. At this point, a finer granularity search is performed in the neighborhood of $p^{(k)}$. It is observed numerically that $R_{sum}(\theta, p)$ monotonically increases as a function of p for a fixed θ, and hence, with a sufficiently low value of Δ, the value of $\tilde{p}(\theta)$ is expected to be close to $p^*(\theta)$. The rotation angle that maximizes $R_{sum}(\theta, \tilde{p}(\theta))$ is then given by

$$\theta' = \arg \max_{\theta} R_{sum}(\theta, \tilde{p}(\theta)). \tag{30}$$

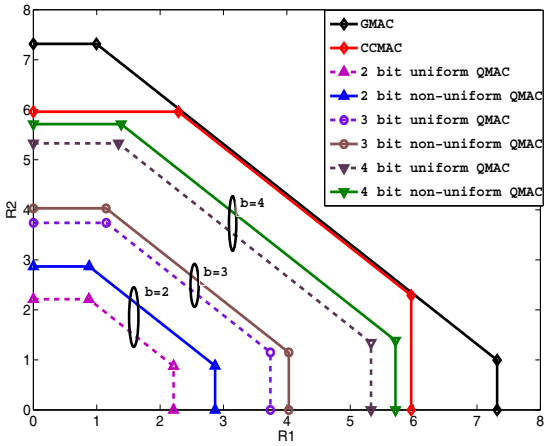

Fig. 5. Comparison between the achievable rate regions with uniform and non-uniform receiver quantization for a two-user MAC. User 1 uses a 64-QAM signal set and User 2 uses the optimally rotated 64-QAM. SNR per user = 22 dB.

B. Results and Discussion

We compute the rate regions achieved by the proposed non-uniform quantizer for a two-user QMAC with User 1 using a QAM alphabet and User 2 using the optimally rotated QAM, and compare them with those achieved by the uniform quantizer. Figure 5 shows the rate regions for 64-QAM at SNR per user = 22 dB, and Fig. 6 shows the rate regions for 16-QAM at SNR per user = 15 dB. From Fig. 5, we observe that the maximum achievable sum rate with a $b = 2$-bit uniform quantizer is 3.0891 bits, whereas a $b = 2$-bit non-uniform quantizer achieves a sum rate of 3.7486 bits, which is a 21.35% increase in the sum rate. This shows that significant enlargement in the rate region is achieved with non-uniform quantization compared to uniform quantization. Table I presents a summary of the observations from Figs. 5 and 6.

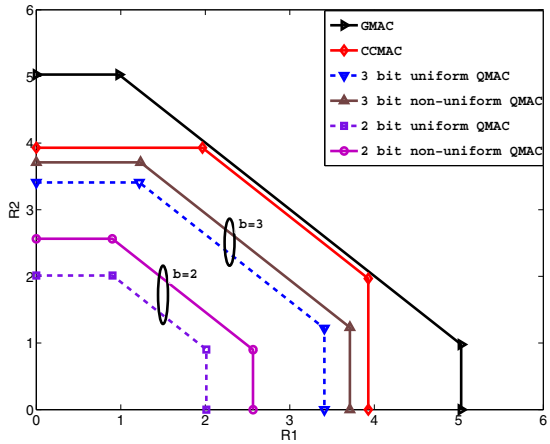

Fig. 6. Comparison between the achievable rate regions with uniform and non-uniform receiver quantization for a two-user MAC. User 1 uses a 16-QAM signal set and User 2 uses the optimally rotated 16-QAM. SNR per user = 15 dB.

# quant. bits, b	Uniform Quantizer	Non-uniform Quantizer		% gain
	$R_{sum}(\theta^{opt})$ (bits)	$R_{sum}(\theta', \tilde{p}(\theta'))$ (bits)	$\tilde{p}(\theta')$	
User 1: 16-QAM, User 2: Optimally rotated 16-QAM (Fig. 6)				
$b = 2$	2.9144	3.4675	2.9	18.98
$b = 3$	4.6290	5.0787	1.3	09.71
User 1: 64-QAM, User 2: Optimally rotated 64-QAM (Fig. 5)				
$b = 2$	3.0891	3.7486	3.2	21.35
$b = 3$	4.8910	5.1790	1.6	05.89

TABLE I
COMPARISON OF THE MAXIMUM ACHIEVABLE SUM RATES WITH UNIFORM AND NON-UNIFORM RECEIVER QUANTIZATION FOR A TWO-USER QMAC

VI. CONCLUSIONS

We investigated the effect of receiver quantization on the achievable rate region of Gaussian MAC with finite input alphabet. Low-precision quantization was shown to significantly degrade the rate region. Uniform quantization was found to result in significant rate loss due to the dense distribution of the sum signal set near the origin. So we proposed a non-uniform quantizer that achieved significant enlargement of the rate region compared to a uniform quantizer. As a further extension to this study, design of optimum non-uniform quantizer that will attain the maximum achievable sum rate for a given quantization resolution can be investigated.

REFERENCES

[1] R. H. Walden, *ADC Survey and Analysis*, *IEEE Jl. Sel. Areas in Commun.*, vol. 17, no. 4, pp. 539-550, April 1999.
[2] G. Middleton and A. Sabharwal, "On the impact of finite receiver resolution in fading channels," *Allerton Conf. on Communication, Control and Computing*, September 2006.
[3] J. Singh, O. Dabeer, and U. Madhow, "On the limits of communication with low-precision analog-to-digital conversion at the receiver," *IEEE Tran. Commun.*, vol. 52, no. 12, pp. 3629-3639, December 2009.
[4] T. M. Cover and J. A. Thomas, *Elements of Information Theory*, 2nd Edition, Wiley Series in Telecommmun. and Sig. Proc., 1999.
[5] J. Harshan and B. Sundar Rajan, "Finite signal-set capacity of two-user Gaussian multiple access channel," *Proc. IEEE ISIT'2008*, pp. 1203-1207, July 2008.
[6] J. A. Nossek and M. T. Ivrlač, "Capacity and coding for quantized MIMO systems," Proc. IWCMC'06, pp. 1387-1392, 2006.